European Review for Medical and Pharmacological Sciences 2023; 27: 4254-4268

Raspberry ketone glucoside suppresses melanin synthesis through *IL6/JAK1/STAT3* signal pathway

Q.-Q. GUO[1], Y.-Y. YUAN[1], T.-W. SUN[1], S.-J. WU[1], X.-H. LI[2], H.-S. ZHAO[2]

[1]School of Chemical Engineering and Light Industry, Guangdong University of Technology, Guangzhou, China
[2]Guangdong Provincial Key Laboratory of South China Structural Heart Disease, Guangdong Cardiovascular Institute, Guangdong Provincial People's Hospital, Guangdong Academy of Medical Sciences, Guangzhou, China

Abstract. – OBJECTIVE: This study aimed to evaluate the anti-melanogenic activity of raspberry ketone glucoside (RKG) and further explore the specific molecular mechanisms by which RKG affects melanogenesis.

MATERIALS AND METHODS: The B16F10 cells model, the mushroom tyrosinase model and the zebrafish model were used to assess the whitening activity of RKG. We subsequently identified possible pathways related to RKG inhibition of melanogenesis by RNA-seq analysis and qRT-PCR on the zebrafish model, and further explored the effects of key genes on the pathway on the melanogenic effect of RKG by using related pathway inhibitors and Tg [mpeg: EGFP] transgenic zebrafish line.

RESULTS: RKG could noticeably inhibit melanogenesis in B16F10 cells *in vitro* and on zebrafish *in vivo*. The RNA-Seq analysis and the qRT-PCR in zebrafish embryos indicated that the inhibition of melanogenesis by RKG could be achieved by activating *JAK1/STAT3* signal pathway and inhibiting the expression levels of the *MITFa, TYR, TYRP1a* genes directly associated with melanogenesis. The inhibitor tests revealed that the inhibitory effect of the RKG on melanogenesis was restored by the *IL6, JAK1/2*, and *STAT3* inhibitors, specifically *STAT3* inhibitor. We further examine the relationship between the *JAK1/STAT3* signal pathway and the *MITFa*. The achieved results indicate that the RKG could activate the zebrafish macrophages *via* the *JAK1*, but the inhibition of macrophage activation by loganin did not affect the anti-pigmentation effect of the RKG.

CONCLUSIONS: RKG showed remarkable whitening activity on both B16F10 cells *in vitro* and zebrafish model *in vivo*. Furthermore, RKG could inhibit melanogenesis by activating the *IL6/JAK1/STAT3* pathway, inhibiting the transcriptional activity of *MITFa*, and its downstream expression levels of the *TYR* and *TYRP1a* genes.

Key Words:
Raspberry ketone glucoside (RKG), Melanogenesis, *IL6/JAK1/STAT3* signal pathway, Zebrafish.

Introduction

Skin whitening agents are capable of lightening the skin color and have a tremendous market in Asia[1], but common whitening agents such as hydroquinone, kojic acid, and arbutin, have been reported to take potential risks for side effects, including dermatitis, cytotoxicity, and cancer[2]. Therefore, it is of great significance to search for new kinds of whiting agents. Raspberry ketone glucoside (RKG; p-hydroxyphenyl-2-butanone-β-D-glucoside), as an active ingredient extracted from the raspberry fruit, can be used as an additive to beverages and food products, and has been listed as a whitening ingredient for cosmetics in some regions[3]. However, the whitening activity and the specific molecular mechanism of action of RKG lack clear experimental support. In a study, Ikemoto et al[4] reported that RKG could inhibit melanogenesis in B16 cells *in vitro*, but the whitening activity of RKG *in vivo* and the mechanism of melanogenesis inhibition by RKG were not further investigated.

Melanin is produced by melanocytes that are derived from the neural crest[5], and its generation involves a complex signal gene regulatory network[6]. Three genes are closely related to melanogenesis, tyrosinase (*TYR*), tyrosinase-related protein 1 (*TYRP1a*), and dopachrome tautomerase (*DCT*), which are transcriptionally regulated by the microphthalmia transcription factor (*MITFa*)[7]. The performed explorations have illustrated that inflammatory cytokines and other mediators affect melanogenesis[8]. For instance, interleukin-1 (*IL-1*), interleukin-4 (*IL-4*), interleukin-6 (*IL-6*), interleukin-17 (*IL-17*), and tumor necrosis factor-α (*TNF-α*) could inhibit melanogenesis, while interleukin-10 (*IL-10*), interleukin-18 (*IL-18*), interleukin-33 (*IL-33*), and granulocyte-macrophage colony-stimulating factor (*GM-CSF*) are capable of promoting melanogenesis[9-12]. Recently, the Janus

Corresponding Author: Hia-Shan Zhao, Ph.D; e-mail: hartzhao@163.com

kinase (*JAK*)/signal transducer and activator of transcription (*STAT*) signal pathway associated with the *IL*-6 family[13] is known to be involved in melanin synthesis. The *JAK/STAT* signal pathway regulates a variety of biological processes, including cell proliferation, differentiation, and apoptosis[14,15]. It is reported[16,17] that the *JAK/STAT* signal pathway plays a specific role in skin pigmentation-related disorders such as vitiligo and melanoma. Some cytokines and active ingredients have also been reported to regulate melanogenesis in normal human melanocytes *via* the *JAK/STAT* signal pathway[18-21].

In the present investigation, we first examined the whitening activity of the RKG in B16F10 cells *in vitro* and zebrafish models *in vivo*, and after that, we further investigated the molecular mechanism of melanogenesis inhibition activity by the RKG by RNA-seq, qRT-PCR, and inhibitor tests. These results provide evidence that the RKG acts as a whitening agent and helps us appreciate the molecular mechanism by which RKG inhibits melanogenesis.

Materials and Methods

Chemical Teagents

RKG (CAS: 537-42-8; purity ≥98%) and polyphenol oxidase (mushroom tyrosinase, CAS: 9002-10-2; 1100 U/mg) were purchased from Yuanye Bio-Technology (Shanghai, China). α-arbutin (CAS: 84380-01-8; purity ≥99%) was obtained from Teelar Bio-technology (Guangzhou, China). L-DOPA (CAS: 59-92-7; purity≥99%) and L-Tyrosine (CAS: 60-18-4; purity: 99%) were purchased from Aladdin (Shanghai, China). Static (SC, CAS: 19983-44-9; purity: 98.92%), LMT-28 (CAS: 1239600-18-0; purity: 98.85%), ruxolitinib (RB, CAS: 941678-49-5; purity: 99.83%), and loganin (CAS: 18524-94-2; purity: 99.82%) were obtained from MedChemExpress LLC (Shanghai, China). Other chemicals and reagents used were of analytical grade.

Cell Culture

The murine B16F10 melanoma cell line was purchased from BNCC (Beijing, China), cultured at 37°C in the presence of a moist 5% CO_2 incubator in DMEM medium (Gibco, Grand Island, NY, USA), and supplemented with 10% (v/v) heat-inactivated fetal calf serum (FBS, ExCell Bio, China), penicillin (100 U/mL), and streptomycin (100 g/mL) (Gibco, Grand Island, NY, USA).

Cell Viability Assay

The cell viability was assessed using a CCK8 Cell Counting Kit (Trans Gen, Beijing, China) according to the manufacturer's instructions per the previous description[22].

Cell Tyrosinase Activity and Melanin Content Assay

Tyrosinase activity and melanin content assay were determined as described with minor modifications[23]. The cells were seeded into six-well plates and incubated at a density of 3×10^5 for 24 hours, and the medium was removed and placed in a fresh medium containing various concentrations of RKG for an additional 48 hours. The cells were washed with Phosphate-buffered saline (PBS) solution (PH=6.8, Leagene Bio, Shanghai, China) and were lysed by implementing a Total Protein Extraction Kit (BestBio, Shanghai, China) to obtain the supernatant for tyrosinase activity assays and the precipitation for melanin content assays. A portion of the resulting total protein solution was employed in the BCA Protein Quantitative Kit (BestBio) to achieve total protein levels, and a fraction was utilized for measuring the tyrosinase activity by employing L-DOPA oxidation[24]. 150 μL L-DOPA (1 mg/mL) and 50 μL of supernatant were added to 96-well plates and incubated at a dark chamber of 37°C for 30 min, and the absorbance at 475 nm was determined *via* a plate reader (TriStar2 LB942, Germany). The absorbance per microgram of the protein (A/μg) represents the relative cell tyrosinase activity. It was the relative percentage content of the control.

The total melanin oven in the cell precipitate was dried and resuspended in 60 μL 1 N NaOH, and in a 95°C metal bath for 30 min. After cooling, the absorbance at 405 nm was measured by means of 1 N NaOH solution as a background, the absorbance per microgram of the protein (A/μg) denotes the relative melanin content. It was the relative percentage content of the control. All the experiments were conducted at least three times with similar results.

Mushroom Tyrosine Activity Assay

The tyrosinase enzyme inhibition experiment using L-Tyrosine as substrate and mushroom tyrosinase as enzyme source was performed to assess the inhibitory effect of the RKG on the mushroom tyrosinase activity[25]. 40 μL L-Tyrosine (0.5 mg/mL), 40 μL gradient concentration RKG, and 30 μL PBS (PH=6.8) were then added to the 96-well plate in sequential order, fully mixed, incubated at 37°C at constant temperature

for 10 min before successively adding 20 μL mushroom tyrosinase (500 U/mL) in each well, and then all drugs were diluted in PBS (PH=6.8). The tyrosinase activity was measured at 475 nm, representing the relative percentage content of the control.

Zebrafish Maintenance and Ethic Statements

The zebrafish were raised and maintained in accordance with the standard procedure[22]. Wild-type AB stock and transgenic zebrafish line with fluorescent labeled macrophages Tg [mpeg: EGFP] were purchased from China Zebrafish Resource Center (Wuhan, China).

Acute Toxicity Test of the Zebrafish

The 24 hours post-fertilization (hpf) synchronized embryos were collected in 96-well plates, and the zebrafish embryo acute toxicity assay[26] was exploited to determine the toxicity within 96 hours. During the course of the present research, we modified some testing conditions to meet our objectives. In each well, one embryo was treated with 12 biological replicates. Holt Buffer[27] was utilized for various concentrations of the RKG or α-arbutin. The consisting control groups were exposed to the Holt Buffer as described. At 48, 72, and 96 hpf, the viability of embryos was assessed based on the number of live and dead embryos. All tests were independently conducted in duplicate.

Zebrafish Body Surface Melanin Quantification Test

The synchronized zebrafish embryos were collected by accounting for 15 embryos per well in 24-well plates containing 1 mL of the Holt Buffer. The RKG was dissolved in the Holt Buffer. The experimental zebrafish were exposed to varying concentrations of the RKG from 24 to 72 hpf, while the buffer was exploited as a control. The embryos were subsequently fixed on glass slides with 4% methylcellulose (Yuanye, Shanghai, China), and the melanin phenotype was recorded by employing an upright microscope (Axio Lab. A1, Carl Zeiss, Germany). Dorsal view image data were imported into the ImageJ software (version, V1.53q) to quantify the relative phenotype melanin content of zebrafish embryos. The relative phenotype melanin content was evaluated as a percentage of the control. All the trials were performed at least three times with similar results.

Zebrafish Tyrosinase Activity and Melanin Content Assay

Zebrafish tyrosinase activity and melanin content determination were consistent with the prior cell processing procedure, except for the pretreatment procedure. Synchronized 24 hpf embryos were collected in 24-well plates, 15 embryos/well, and exposed to various concentrations of RKG until 72 hpf. Embryos were collected with 1.5 mL EP tubes and washed with PBS (PH=6.8). All the experiments were conducted at least three times with similar results.

RNA Isolation, cDNA Library Preparation, and RNA-Seq

Total RNA was extracted from 72 hpf zebrafish embryos collected at various concentrations by utilizing the Total RNA Isolation Kit (RC101, Vazyme, Nanjing, China), according to the manufacturer's protocol. Assays of total RNA quality were carried out on an Agilent 2100 Bioanalyzer (Agilent, CA, USA), agarose gel electrophoresis, and nanophotometer. The first strand of cDNA was synthesized in the M-MuLV reverse transcriptase system using fragmented mRNA as a template and casual oligonucleotide as a primer, and the RNA strand was subsequently degraded with RNaseH. Further, the second strand of cDNA was synthesized from dNTPs in the presence of the DNA polymerase I system. The purified double-stranded cDNA underwent end repair, a tail, and ligation of sequencing adaptors to finally establish 12 cDNA libraries consisting of three repeats in each set and were sequenced in paired-end 150 bp mode using the Illumina HiseqTM 2500/4000 platform. RNA library sequencing was assisted by Gene Denovo Biotechnology, Ltd (Guangzhou, China).

Global and Differential Gene Expression Analysis

The differential expression analysis was conducted using DESeq2[28], and the differentially expressed genes (DEGs) were selected according to the fold change greater than 1.5 and p-value less than 0.05. The functions of genes with significantly differentially expressed manners were classified based on the KEGG[29] database. The KEGG pathways with a p-value less than 0.05 were considered and remarkably enriched.

RNA Isolation, cDNA Synthesis and Quantitative Real-Time Polymerase Chain Reaction (qRT-PCR)

RNA isolation was performed employing Total RNA Isolation Kit of 72 hpf zebrafish embryos as previously described. The HiSuper®

III RT SuperMix for qPCR (RC323-01, Vazyme, Nanjing, China) is employed for cDNA synthesis. The qRT-PCR was performed by means of ChamQ Universal SYBR qPCR Master Mix (Vazyme, Nanjing, China) and self-designed primers (refer to the primer sequence in **Supplementary Table I**). A StepOnePlus Real-Time PCR system (Applied Biosystems, Foster City, CA, USA) was implemented to perform PCR in triplicate for each RNA sample with 0.5 μL of cDNA and 10 μL of 2X ChamQ Universal SYBR qPCR Master Mix. The relative mRNA expression levels were evaluated by utilizing the $2^{-\Delta\Delta Ct}$ formula, and β-actin gene expression was then normalized to target gene expression.

Statistical Analysis

Statistical analysis was performed using GraphPad Prism 8 (GraphPad Software Inc., La Jolla, CA, USA). All data were presented as mean ± S.D. One-way ANOVA was used to count for significant differences between multiple groups, Student's *t*-test was used to determine the differences between each group. *p*-values less than 0.05 were considered statistically significant.

Results

Effect of the RKG on the Melanin Content and Tyrosinase Activity in B16F10 Cells

CCK8 tests revealed that when the concentration of the RKG reached 25 mM, the growth of B16F10 cells was inhibited, while 15 mM RKG exhibited no effect on the growth of B16F10 cells (i.e., no increase or decrease in the number of cells was detected; see **Supplementary Figure 1A**). As a result, the concentration of the RKG was set to less than 15 mM in all subsequent experiments.

The obtained results indicated that the non-toxic RKG treatment altered the color of B16F10 cells to lighten them (Figure 1A) and noticeably inhibited B16F10 cell melanin content (Figure 1B). Nevertheless, at the corresponding concentration, the RKG did not have a remarkable inhibition of intracellular tyrosinase activity (**Supplementary Figure 1B**), indicating that the anti-melanogenic activity of the RKG *in vitro* models could not be achieved by direct inhibition of cellular tyrosinase activity.

Effect of the RKG on the Melanin Content and Tyrosinase Activity in The Zebrafish Model

After verifying that the RKG could inhibit B16F10 Cells melanogenesis *in vitro*, we performed an *in vivo* zebrafish assay to examine the anti-melanogenic activity of the target compound. First, we tested RKG for acute toxicity in zebrafish embryos, finding that zebrafish embryos survived better at 48, 72, and 96 hpf than α-arbutin. A commonly exploited whitening agent (**Supplementary Figure 2**), and the LC_{50} (median lethal concentration) of the RKG was larger than α-arbutin in all three time periods. Among them, at 72 hpf, the LC_{50} of the RKG was 442.578 mM, which was about 1.6 times that of α-arbutin (**Supplementary Table II**). The results obtained above indicate that the RKG possesses high safety in the zebrafish model.

The phenotypic validity of the melanin in the zebrafish embryos at 72 hpf was observed by analyzing the body pigments *via* an upright microscope. The achieved results demonstrated that the non-toxic RKG concentration could considerably inhibit the phenotype of melanin in 72 hpf zebrafish embryos, reaching about 12% at 5 mM compared to the non-treated zebrafish embryos (Figures 1C and 1D). Embryos at the corresponding concentrations were lysed to determine the melanin content and tyrosinase activity *in vivo*. The obtained results indicated that the zebrafish internal melanin content and the tyrosinase activity were noticeably reduced by the RKG at 0.2, 5-, and 125-mM concentrations compared to the non-treated zebrafish embryos (Figures 1E and 1F).

Overview of the RNA-seq Data

To identify potential signal pathways pertinent to the inhibition of melanin production by the RKG, we first performed a screen for differential genes using DESeq2. The paired comparisons in the three groups identified the same number of genes (26,529), including 25,116 known genes and 1,413 new genes (**Supplementary Table III**). In the comparison of blank to 0.2 mM, blank to 5 mM, and blank to 125 mM, 859, 2484, and 2499 DEGs were identified. In these DEGs, 615, 1274, and 1495 were up-regulated, and 244, 1210, and 1004 were down-regulated, respectively (**Supplementary Figure 3**). Pearson's correlation coefficient (R^2) for sample expression was in the range of 99.6-99.8% for blank-1, blank-2, and blank-3, 99.8-99.9% for 0.2 mM-1, 0.2 mM-2, and 0.2 mM-3, in the interval of 99.7-99.8% for 5 mM-1, 5 mM-2, and 5 mM-3, and in the range of 99.5-99.9% for 125 mM-1, 125 mM-2, and 125 mM-3 (**Supplementary Figure 3**). The volcano scatter plots

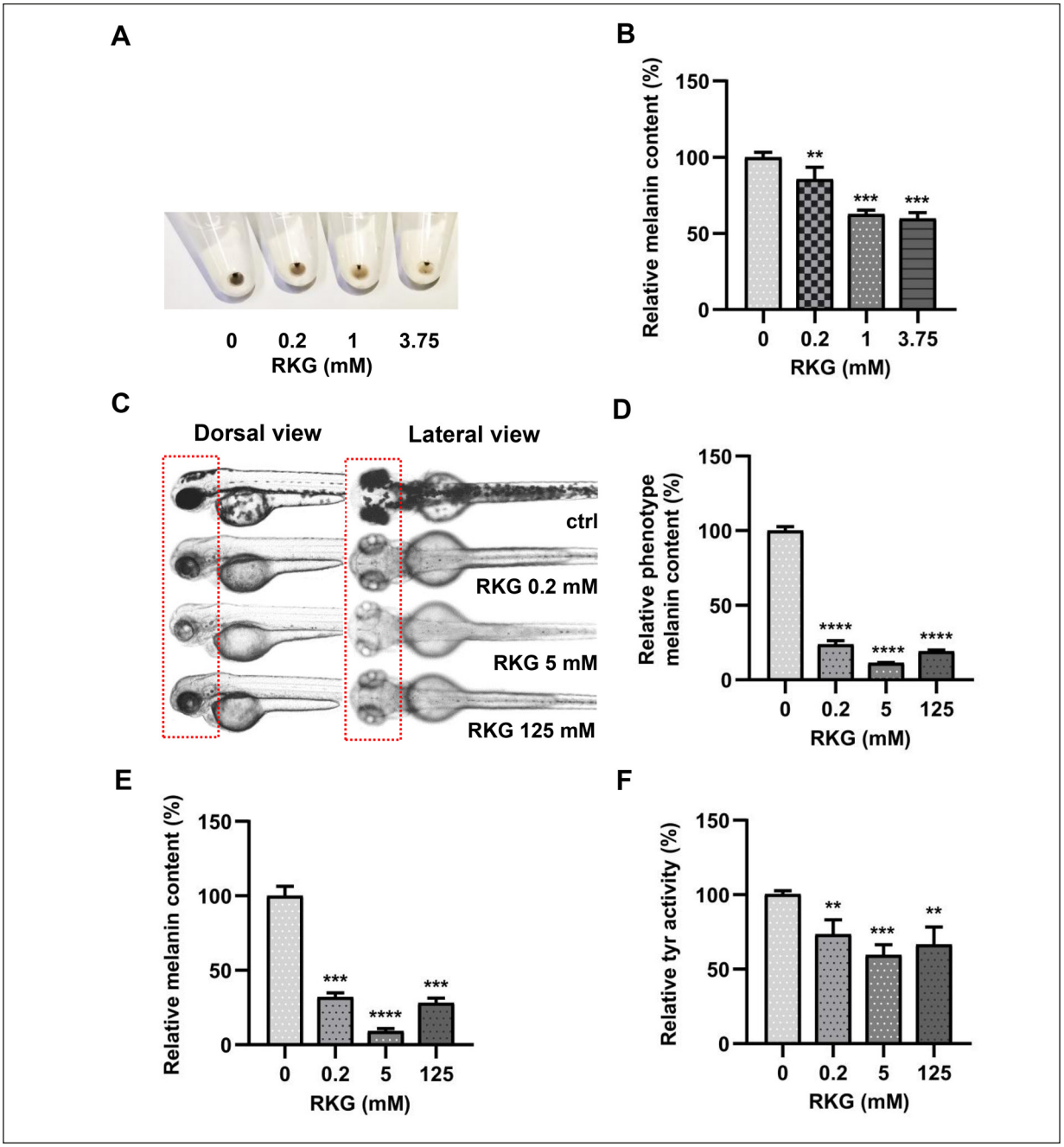

Figure 1. Effect of B16F10 cells *in vitro* and the zebrafish model in vivo on the whitening activity of RKG: (**A**) the photos of B16F10 cells color of samples from (**B**), (**B**) relative melanin content in B16F10 cells treated with different concentrations of RKG, (**C**) effect of RKG on the melanin phenotype in 72 hpf zebrafish embryos, (**D**) the imageJ relative quantification results of dorsal view photographs of zebrafish embryos from (**C**), (**E**) effect of the RKG on melanin content in 72 hpf zebrafish embryos, (**F**) effect of the RKG on tyrosine activity *in vivo* in 72 hpf zebrafish embryos (note: ** $p<0.01$, *** $p<0.001$, **** $p<0.0001$; compared *vs.* non-treated cells or zebrafish embryos; error bars, S.D.).

illustrate the variations in these DEGs (**Supplementary Figure 3**). These results revealed that the sequencing data generated in the present investigation were reliable and could be employed for further analysis.

Differential Gene Expression Analysis

KEGG pathway enrichment analysis was subsequently performed on these DEGs. According to the KEGG database's first- and second-tier classifications, pathways enriched for, and genes

included were counted (**Supplementary Table IV**). The achieved results indicated that in the top 15 of KEGG enrichment, a large number of DEGs were enriched in pathways associated with the endocrine system in organismal systems and signal transduction system in environmental information processing (Figure 2A and 2B). This issue reveals that the mechanism of RKG-inhibited melanogenesis is closely related to pathways related to the endocrine and signal transduction systems.

The enrichment plots specified by circle markers revealed that in the endocrine system, the most enriched pathway is that associated with melanogenesis (ko04916, p=3.60E-05), which is directly related to melanogenesis. In the signal transduction system, the most enriched pathway is the *JAK/STAT* signal pathway (ko04630, p=5.67E-06) (Figure 2C and 2A). As we have previously explained, there exist many reports[18-21] demonstrating that the *JAK/STAT* signal pathway is involved in the mechanisms of inhibiting or promoting melanogenesis through its activation by cytokines or active components.

qRT-PCR Validation

The relative expression level heatmap and qRT-PCR of the melanogenesis pathway-related DEGs results indicated that the expression levels of key genes such as *MITFa, TYR*, and *TYRP1a* were remarkably lessened and consistent with the melanin phenotype in zebrafish embryos (Figure 3A-3D). The relative expression heatmap of key genes related to the *JAK/STAT* signal pathway and the qRT-PCR results illustrated that the expression levels of *IL6*, signaling subunit glycoprotein 130 (*GP130, IL6ST*), Janus kinase 1 (*JAK1*), signal transducer and activator of transcription 3 (*STAT3*), and suppressor of cytokine signaling 3 (*SOCS3b*) were up-regulated (Figure 4A-4F). The results mentioned above reveal that the mechanism by which the RKG suppresses melanogenesis is closely related to melanogenesis and *IL6/JAK1/STAT3* pathways.

The IL6/JAK1/STAT3 Signal Pathway Related Inhibitors Attenuated the Inhibitory Effect of RKG on Melanogenesis in Zebrafish Embryos

To further verify whether the *IL6/JAK1/STAT3* pathway is involved in the molecular mechanism of RKG inhibiting melanogenesis, synchronized zebrafish embryos treated with RKG were cotreated with 15 μM stattic (*STAT3* target)[30], 15 μM LMT-28 (*GP130* target)[31], and 15 μM ruxolitinib (*JAK1/2* target)[32], respectively (Figure 5A). Melanin phenotype was recorded from 24 to 72 hpf. According to the achieved results, the inhibitor-treated groups of zebrafish embryos had a deeper melanin phenotype compared to the RKG 200 μM group (Figure 5B). This fact proves our conjecture that the RKG inhibits melanogenesis *via* the activation of the *IL6/JAK/STAT* pathway.

Independency of the Melanogenesis from RKG-activating macrophages

It was reported that the *JAK/STAT* signal pathway activation would be capable of promoting macrophage activation[33-35] and inducing inflammation. Additionally, macrophages were reported to be involved in melanogenesis in melanocytes through paracrine effects[36]. The macrophage fluorescent-labeled zebrafish embryos, *JAK1/2* inhibitor, and macrophage activation inhibitor loganin[37,38] were exploited to clarify how *JAK1/STAT3* signal pathway affects melanogenesis in the zebrafish. Macrophage fluorescent-labeled zebrafish treated with RKG were cotreated with ruxolitinib and loganin from 24 to 72 hpf. Photographs were taken by means of a fluorescence upright microscope, and fluorescent macrophages with end-to-tail yolk in 72 hpf zebrafish embryos were counted by employing ImageJ software. The obtained result revealed that the RKG could activate macrophages in zebrafish embryos and ruxolitinib could inhibit this phenomenon (Figure 6A and 6B). Then, to verify whether the activated macrophages inhibit melanogenesis in zebrafish embryos, synchronized zebrafish embryos were treated with the RKG and loganin. The achieved results illustrated that loganin did not affect melanogenesis in the zebrafish. It implies that the RKG could activate macrophages in the zebrafish embryos but did not affect embryonic melanogenesis (Figure 6C and 6D).

Discussion

Previous explorations[3] revealed that RKG has a whitening activity and could be utilized as a whitening agent in cosmetic products. Nevertheless, the mechanism by which the RKG inhibits melanin production has not been fully elucidated. To the best of our knowledge, only one study examined whether the RKG could inhibit melanogenesis, while this research only employs the B16 cells *in vitro* for activity evaluation, and not involved the mechanism of direct inhibition of

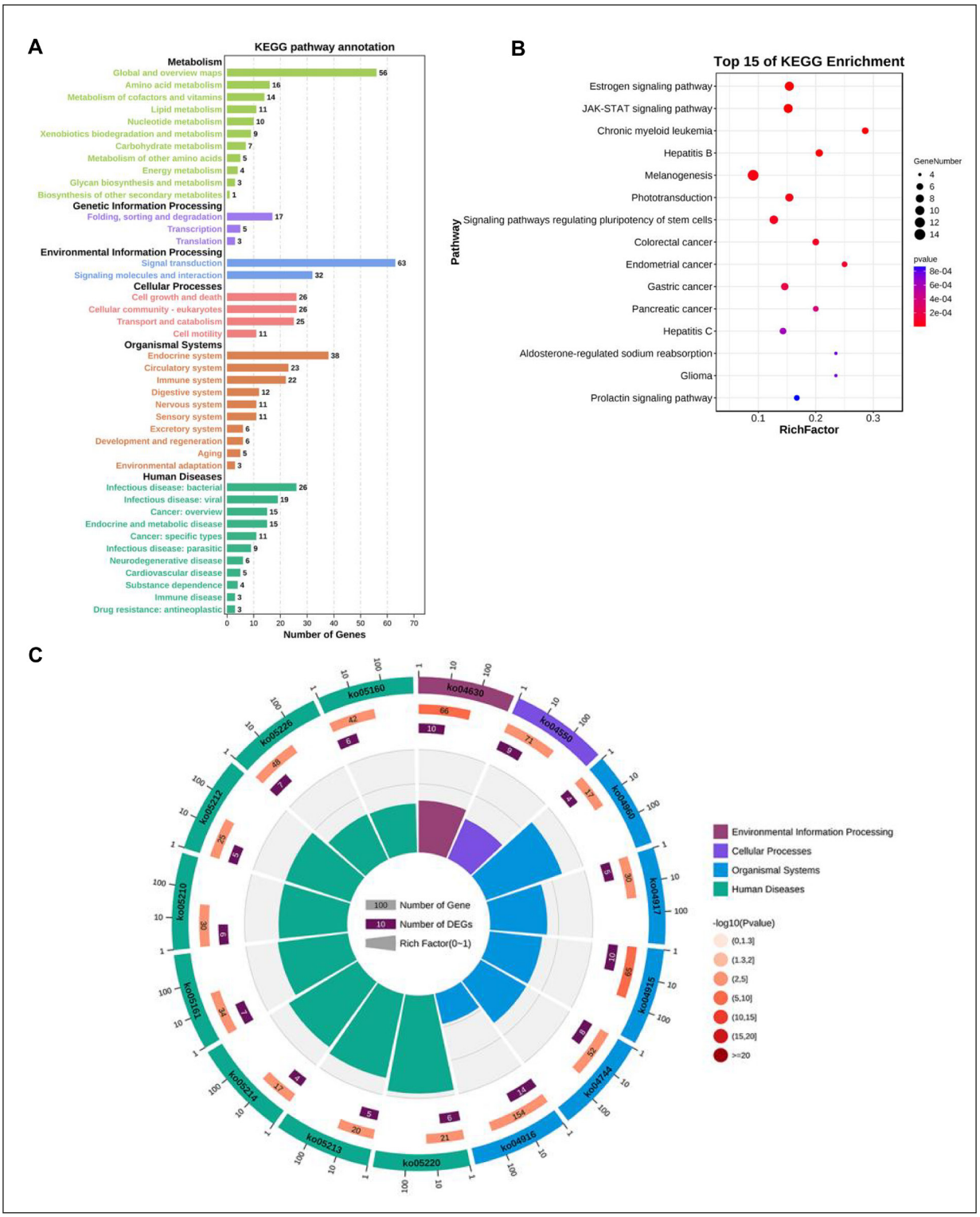

Figure 2. Differential gene expression analysis: (**A**) statistical plot of the grade B classification of each pathway of the differentially enriched genes, (**B**) bubble diagram of the top 15 noticeably enriched pathways. The graph is plotted with *p*-values of significance for various pathways. The abscissa denotes the gene-rich factor (i.e., the number of differential genes enriched to the current pathway/the number of that species enriched to the current pathway), and the ordinate represents the pathway. Bubble size represents the number of genes enriched in different pathways, and bubble color represents the degree of enrichment in different pathways, (**C**) circle-marker plots of the top 15 significantly enriched differential pathways. Outside the circle is a sitting ruler of the gene number. Different colors represent different KEGG A Class.

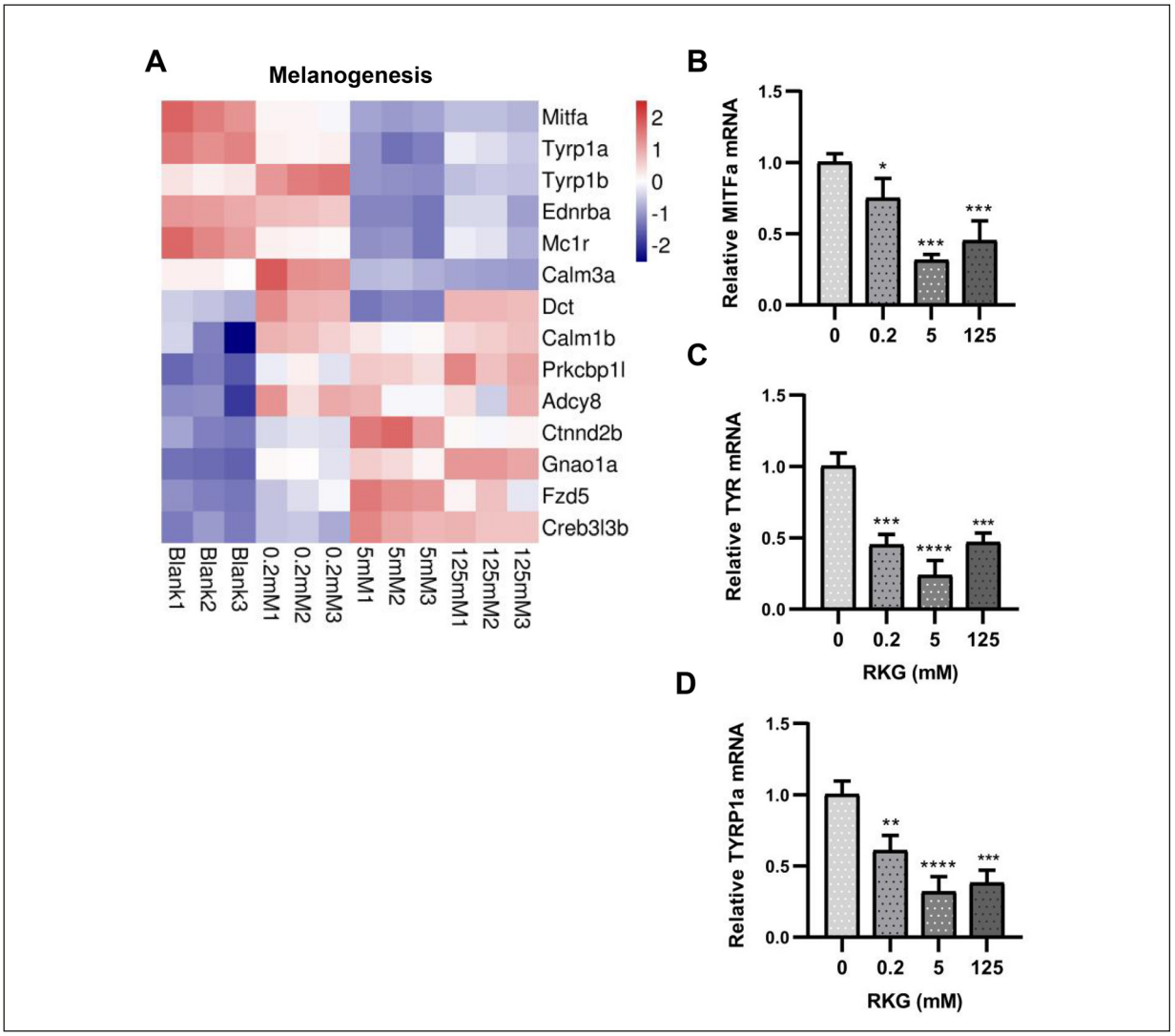

Figure 3. The qRT-PCR validation results of differential genes related to the melanogenesis pathway: (**A**) heatmap of relative expression of differential genes pertinent to the melanogenesis pathway, (**B-D**) qRT-PCR validation results of differential genes related to the melanogenesis pathway (note: * $p<0.05$, ** $p<0.01$, *** $p<0.001$, **** $p<0.0001$; compared *vs.* non-treated groups; error bars, S.D.).

melanogenesis activity by the RKG[4]. Therefore, the *in vivo* test and the mechanism study are required to further support the conclusions of the current study. In our research works, we comprehensively explored the whitening activity of the RKG as well as the specific molecular mechanism of its inhibition of melanogenesis (Figure 7).

The first crucial point of our study is that the RKG has excellent anti-melanin activity, which could significantly inhibit melanogenesis in both B16F10 cells *in vitro* and zebrafish *in vivo*. In addition, compared to α-arbutin, a well-known anti-pigmentation reagent[39], the RKG has a higher safety/effective window in the zebrafish model, which indicates great potential for application (**Supplementary Figure 4** and **Supplementary Table V**). Meanwhile, the results obtained by the tyrosinase activity assay indicated that the RKG only inhibited the tyrosinase activity in the zebrafish model *in vivo* (Figure 1F), but not in either B16F10 cells or mushroom tyrosinase *in vitro* (**Supplementary Figure 5**). This fact indicates that the anti-melanin activity of the RKG was not achieved by the direct inhibition of the tyrosinase activity but exist other molecular mechanisms of action.

To further realize the specific molecular mechanism involved in RKG-mediated melanogenesis reduction, zebrafish embryos treated with the RKG were subjected to transcriptome analysis. By the KEGG enrichment analysis and the qRT-PCR

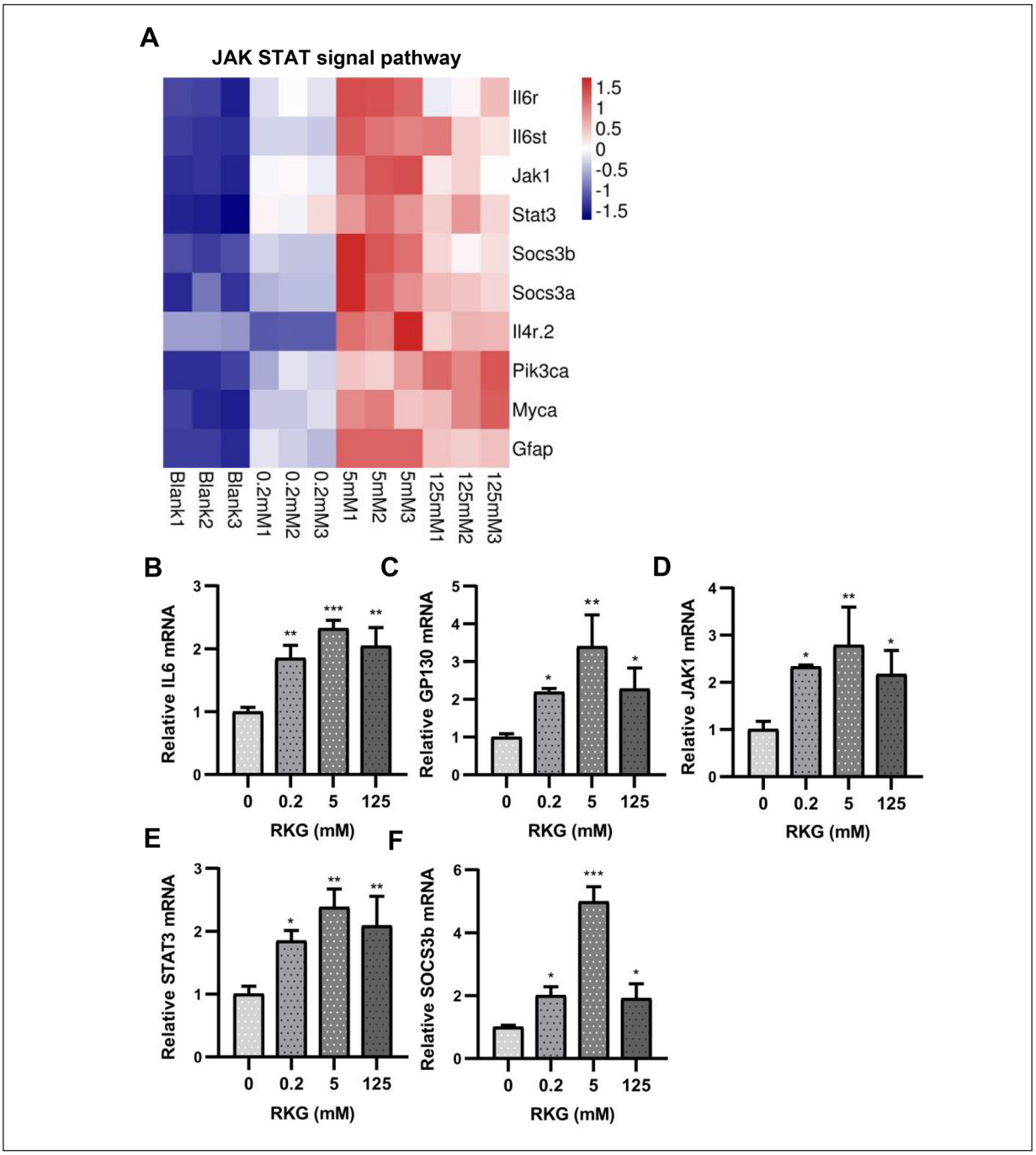

Figure 4. The qRT-PCR validation results of differential genes related to the *JAK/STAT* pathway: (**A**) heatmap of relative expression of genes associated with the *JAK/STAT* pathway, (**B-F**) qRT-PCR validation results of differential genes related to the *JAK/STAT* pathway (note: * $p<0.05$, ** $p<0.01$, *** $p<0.001$; compared *vs.* non-treated groups; error bars, S.D.).

validation, we found a substantial enrichment of the DEGs associated with the melanogenesis pathway in the RKG-treated zebrafish embryos (Figure 2). This includes *MITFa* (i.e., the most critical transcription factor for melanogenesis), *TYR* (i.e., the rate-limiting enzyme for melanogenesis), and *TYRP1a* (i.e., the acritical enzyme for catalyzing tyrosine metabolism). All three genes exhibit a descending trend and are consistent with the melanin phenotype in zebrafish embryos (Figure 3). This fact suggests that the RKG could influence the melanin production in the zebrafish, by regulating both *MITFa* and its downstream gene expression levels of the *TYR* and *TYRP1a*.

The enrichment analysis results also demonstrated a remarkable enrichment of DEGS related to the *IL6/JAK/STAT* signal pathway (Figure 2), which essentially comprised the *IL6R, GP130, JAK1, STAT3*, and *SOCS3b*, which were all upregulated compared to the control group. The qRT-PCR also indicated that the RKG upregulated the *IL6* gene expression level (Figure 4). *IL-6* has been well-known as a cytokine with anti-melanogenic activity. *IL-6* was first demonstrated to inhibit melanogenesis in melanocytes in 1991[40]. Since then, several investigations have also proved that *IL-6* could inhibit melanogenesis[41], and further explorations revealed that the mechanism of *IL-6* inhibited melanogenesis was chiefly related to the downregulation of the *MITF* expression[42]. The *IL-6* family signaling factors are closely related to the *JAK/STAT* pathways[43]. More importantly, the *IL-6*/*IL-6R* complex binds to the signal transducer *GP130* to activate the *JAK1*. Then, the *STAT3* is phosphorylated and dimerized by the *JAK1*. After this, the *STAT3* could be transported into the nucleus through the nuclear membrane to regulate the expression of related genes, including *SOCS3b* (i.e., a crucial negative regulator of this pathway)[44,45]. The *JAK/STAT* signal pathway was also previously reported to be involved in the regulation of melanogenesis. Cytokines such as interferon-gamma (*IFN-γ*), and interleukin-4 (*IL-4*) inhibit melanogenesis in normal human melanocytes *via* the *JAK/STAT* signal pathway[18,19]. Active components such as Ganoderma lucidum polysaccharides could inhibit melanogenesis *via* the *IL-6/STAT3/FGF2* signal pathway[20], and Agerarin can inhibit melanogenesis *via* the *STAT3* pathway[21] Based on the above analyses, we proposed that the RKG could inhibit melanogenesis in zebrafish *via* the *IL6/JAK1/STAT3* signal pathway. The correlated inhibitors verify our conjecture. In contrast to the 200 μM RKG group, the melanogenic phenotype was all deepened by the LMT-28, *IL-6* inhibitor, RB, *JAK1/2* inhibitor, and SC, the *STAT3* inhibitor in zebrafish embryos. In particular, after inhibiting *STAT3 via* SC, the melanin phenotypes of zebrafish embryos almost completely recover (Figure 5).

But how does the RKG *via* the *IL6/JAK1/STAT3* signal pathway affect melanogenesis in the zebrafish? We believe that there are two possible explanations for this question. The first possible mechanism is that *IL6/JAK1/STAT3* directly inhibits the transcriptional activity of *MITFa* after the RKG treatment, and therefore, is incorporated into the reduction of melanogenesis. It has been

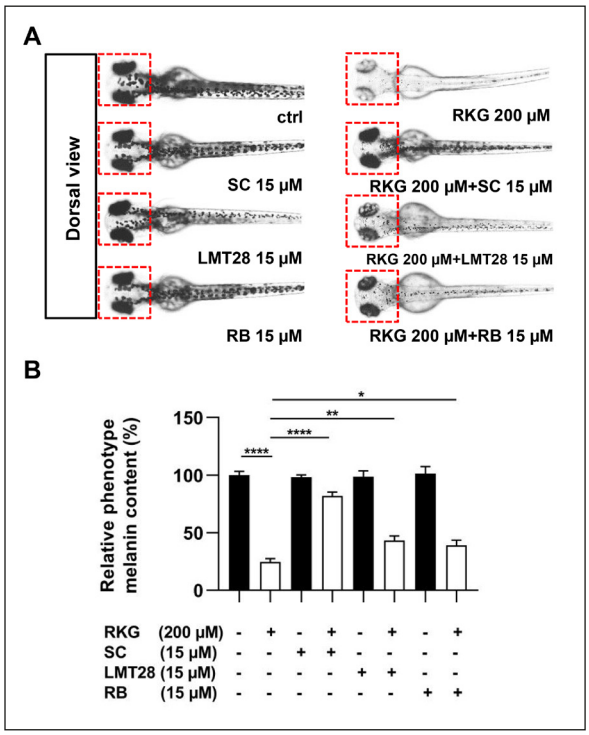

Figure 5. *IL6/JAK/STAT* signal pathway-related inhibitors attenuated the inhibitory effect of the RKG on the melanogenesis in zebrafish embryos: (**A**) dorsal view of the zebrafish embryos co-treated with RKG and the inhibitors, at 72 hpf, (**B**) the imageJ relative quantification results of dorsal view photographs of 72 hpf zebrafish embryos (note: * $p<0.05$, ** $p<0.01$, *** $p<0.001$, **** $p<0.0001$; compared *vs.* 200 μM RKG Group; error bars, S.D.).

reported that the *MITF* is regulated by the *STAT3* in B16 melanoma cells, human cells, and the 3D melanoma model. For instance, in the B16/F10.9 melanoma cells, the *IL-6/IL-6R* chimeras cause rapid phosphorylation of the *STAT3* through the stimulation of GP130. The phosphorylated *STAT3* downregulates *PAX3* and indirectly lessens the *MITF* promoter activity[42]. The results obtained in either mouse or human cells demonstrated that the loss or knockdown of the *STAT3* leads to the upregulation of the *MITF*[46-48]. Our *STAT3* inhibitor experiments illustrated that the *STAT3* did play a critical role in melanogenesis in RKG-treated zebrafish.

The second possible mechanism is that the RKG indirectly inhibits melanogenesis by activating macrophages through the *JAK1/STAT3* signaling pathway. It is reported that the *JAK/STAT3* pathway activation could promote macrophage activation, and the macrophages could produce cytokines to affect melanogenesis through paracrine action[33-36]. To test this conjecture, Tg [mpeg: EGFP] transgenic zebrafish line with fluorescently labeled macrophages

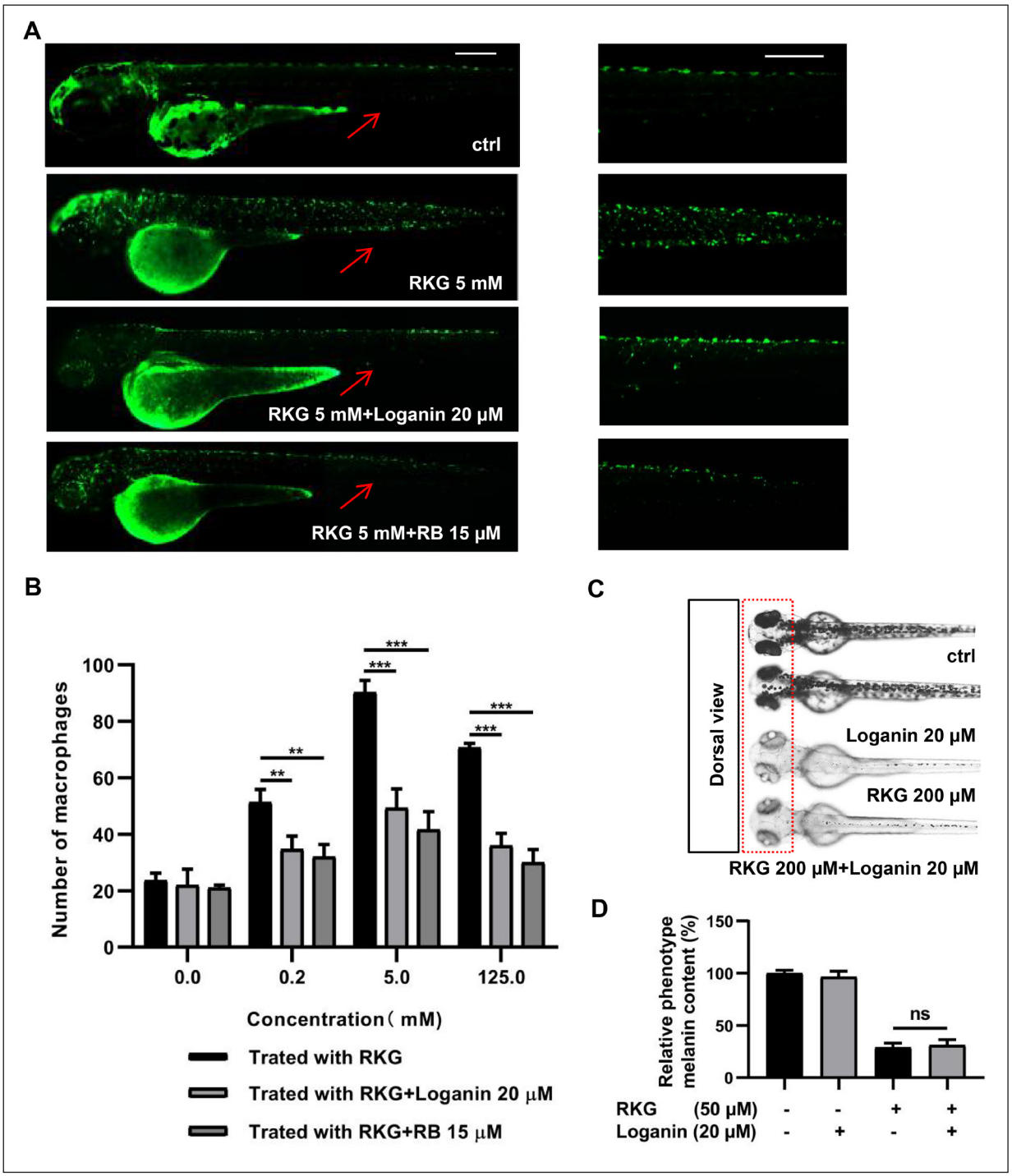

Figure 6. Independence of the melanogenesis from the RKG activating macrophages: (**A**) dorsal view of the 72 hpf macrophage fluorescent-labeled zebrafish embryos co-treated with RKG and loganin or ruxolitinib (note: the red arrow points to the enlarged part and the scale bar is set as 100 μm), (**B**) number statistics of macrophages from the yolk end to the tail of 72 hpf macrophage fluorescent-labeled zebrafish embryos, (**C**) dorsal view of the 72 hpf zebrafish embryos co-treated with the RKG and loganin, (**D**) the imageJ relative quantification results of dorsal view photographs of 72 hpf zebrafish embryos (note: ** $p<0.01$, *** $p<0.001$, **** $p<0.0001$; compared *vs.* RKG treated group; ns $p>0.05$; compared *vs.* 200 μM RKG group; error bars, S.D.).

and macrophage activation inhibitor, loganin were employed. The obtained results revealed that the RKG could activate the zebrafish macrophages *via* the *JAK1*, but the inhibition of macrophage

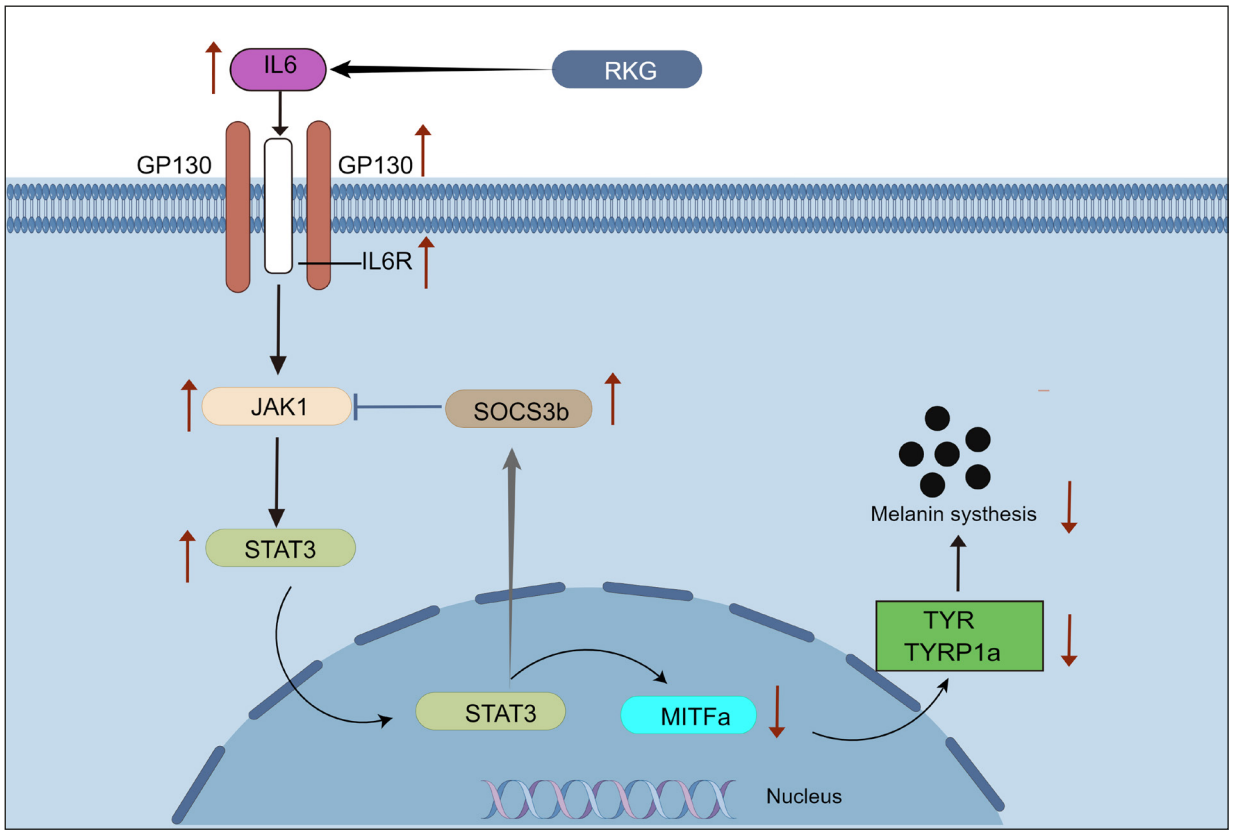

Figure 7. RKG suppresses melanin synthesis through *IL6/JAK1/STAT3* signal pathway (note: red arrow represents the activity of the RKG, while the black arrow specifies the direct stimulatory modification).

activation by loganin did not affect the anti-pigmentation effect of the RKG (Figure 6). Thus, we believed that the RKG could inhibit the transcriptional activity of *MITFa* through the *IL6/JAK1/STAT3* pathway directly, thereby anti-melanogenesis in zebrafish. However, further research is required to realize whether *STAT3* affects gene transcription through the *MITFa* in zebrafish.

Conclusions

In summary, we found that the RKG showed remarkable whitening activity on both B16F10 cells *in vitro* and zebrafish model *in vivo*. Furthermore, the whitening activity of the RKG in zebrafish could be achieved by activating the *IL6/JAK1/STAT3* pathway to inhibit the transcriptional activity of the *MITFa* and then downregulating the expression levels of the *TYR* and *TYRP1a* and ultimately inhibiting the generation of melanin. Our findings provide pieces of evidence for the RKG application in the pigmentation-related industry.

Authors' Contribution

Conceptualization, methodology, data curation, writing-review & editing, supervision, Project administration, funding acquisition, Q.-Q. GUO and H.-S. ZHAO, formal analysis, investigation, writing-original preparation, visualization, Y.-Y. YUAN, Investigation, Validation. T.-W. SUN, Software, Validation, S.-J. WU, Validation, X.-H. LI. All authors have read and agreed to the published version of the manuscript.

Funding

This research was funded by the National Natural Science Foundation of China [grant number 81903600].

Acknowledgments

We thank Institute for Biomedical and Pharmaceutical Sciences for providing the experimental sites and instrumental. We would also like to express our gratitude to EditSprings (https://www.editsprings.cn) for the expert linguistic services provided.

Conflicts of Interest

The authors declare that they have no conflict of interest to declare.

Data Availability Statement

The datasets generated during and/or analyzed during the current study are available in the NCBI Bioproject repository, [PRJNA904835].

Ethics Approval

All procedures performed in the studies involving animals were in accordance with the ethical standards of the Institutional Animal Care and Use Committee of Guangdong Provincial People's Hospital [approval number S2022-010-01].

References

1) Pillaiyar T, Manickam M, Namasivayam V. Skin whitening agents: medicinal chemistry perspective of tyrosinase inhibitors. J Enzyme Inhib Med Chem 2017; 32: 403-425.
2) Bang E, Noh SG, Ha S, Jung HJ, Kim D.H, Lee AK, Hyun MK, Kang D, Lee S, Park C, Moon HR, Chung HY. Evaluation of the Novel Synthetic Tyrosinase Inhibitor (Z)-3-(3-bromo-4-hydroxybenzylidene) thiochroman-4-one (MHY1498) In Vitro and In Silico. Molecules 2018; 23.
3) Li B, Fan B, Fan J, Chang S, Pan X, Wang Y, Wu Y, Song J, He X. Biochemical characterization of an organic solvent-tolerant glycosyltransferase from Bacillus licheniformis PI15 with potential application for raspberry ketone glycoside production. Biotechnol Appl Biochem 2020; 67: 249-256.
4) Yokota T, Ikemoto T, Sasaki M, Toshio Horikoshi. Lasting effect of raspberry ketone glucoside on whitening. Journal of Society of Cosmetic Chemists of Japan 2001; 35: 120-126.
5) Moya Smith, Annabelle Hickman, Dee Amanze, Andrew Lumsden, Peter Thorogood. Trunk Neural Crest Origin of Caudal Fin Mesenchyme in the Zebrafish Brachydanio rerio. Proceedings of the Royal Society of London. Series B: Biological Sciences 1994; 256: 137-145.
6) Hirobe T. How are proliferation and differentiation of melanocytes regulated? Pigment Cell Melanoma Res 2011; 24: 462-478.
7) Dolinska MB, Wingfield PT, Young KN, Sergeev YV. The TYRP1-mediated protection of human tyrosinase activity does not involve stable interactions of tyrosinase domains. Pigment Cell Melanoma Res 2019; 32: 753-765.
8) Zhou S, Zeng H, Huang J, Lei L, Tong X, Li S, Zhou Y, Guo H, Khan M, Luo L, Xiao R, Chen J, Zeng Q. Epigenetic regulation of melanogenesis. Ageing Res Rev 2021; 69: 101349.
9) Fu C, Chen J, Lu J, Yi L, Tong X, Kang L, Pei S, Ouyang Y, Jiang L, Ding Y, Zhao X, Li S, Yang Y, Huang J, Zeng Q. Roles of inflammation factors in melanogenesis (Review). Mol Med Rep 2020; 21: 1421-1430.
10) Choi H, Kim K, Han J, Choi H, Jin SH, Lee EK, Shin DW, Lee TR, Lee A, Noh M. Kojic acid-induced IL-6 production in human keratinocytes plays a role in its anti-melanogenic activity in skin. J Dermatol Sci 2012; 66: 207-215.
11) Zhou J, Shang J, Song J, Ping F. Interleukin-18 augments growth ability of primary human melanocytes by PTEN inactivation through the AKT/NF-kappaB pathway. Int J Biochem Cell Biol 2013; 45: 308-316.
12) Zhou J, Song J, Ping F, Shang J. Enhancement of the p38 MAPK and PKA signaling pathways is associated with the pro-melanogenic activity of Interleukin 33 in primary melanocytes. J Dermatol Sci 2014; 73: 110-116.
13) Schaper F, Rose-John S. Interleukin-6: Biology, signaling and strategies of blockade. Cytokine Growth F R 2015; 26: 475-487.
14) Gutierrez-Hoya A, Soto-Cruz I. Role of the JAK/STAT Pathway in Cervical Cancer: Its Relationship with HPV E6/E7 Oncoproteins. Cells 2020; 9: 2297.
15) Wang GJ, Yang Z, Huai J, Xiang QQ. Pravastatin alleviates oxidative stress and decreases placental trophoblastic cell apoptosis through IL-6/STAT3 signaling pathway in preeclampsia rats. Eur Rev Med Pharmacol Sci 2020; 24: 12955-12962.
16) Hlaca N, Zagar T, Kastelan M, Brajac I, Prpic-Massari L. Current Concepts of Vitiligo Immunopathogenesis. Biomedicines 2022; 10: 1639.
17) Chen J, Huang L, Quan J, Xiang D. TRIM14 regulates melanoma malignancy via PTEN/PI3K/AKT and STAT3 pathways. Aging (Albany NY) 2021; 13: 13225-13238.
18) Su Q, Wang F, Dong Z, Chen M, Cao R. IFN-gamma induces apoptosis in human melanocytes by activating the JAK1/STAT1 signaling pathway. Mol Med Rep 2020; 22: 3111-3116.
19) Choi H, Choi H, Han J, Jin SH, Park JY, Shin DW, Lee TR, Kim K, Lee AY, Noh M. IL-4 inhibits the melanogenesis of normal human melanocytes through the JAK2-STAT6 signaling pathway. J Invest Dermatol 2013; 133: 528-536.
20) Jiang L, Huang J, Lu J, Hu S, Pei S, Ouyang Y, Ding Y, Hu Y, Kang L, Huang L, Xiang H, Zeng Q, Liu L, Chen J, Zeng Q. Ganoderma lucidum polysaccharide reduces melanogenesis by inhibiting the paracrine effects of keratinocytes and fibroblasts via IL-6/STAT3/FGF2 pathway. J Cell Physiol 2019; 234: 22799-22808.
21) Shin SY, Gil HN, Choi JH, Lim Y, Lee YH. Agerarin inhibits alpha-MSH-induced TYR gene transcription via STAT3 suppression independent of CREB-MITF pathway. J Dermatol Sci 2018; 91: 107-110.
22) Guo Q, Wu S, Liang W, Tan J, Liu X, Yuan Y, Li X, Zhao H. Glabrol impurity exacerbates glabridin toxicity in zebrafish embryos by increasing myofibril disorganization. J Ethnopharmacol 2022; 287: 114963.
23) Zhou J, An X, Dong J, Wang Y, Zhong H, Duan L, Ling J, Ping F, Shang J. IL-17 induces cellular stress microenvironment of melanocytes to promote autophagic cell apoptosis in vitiligo. FASEB J 2018; 32: 4899-4916.

24) Yokozawa T, Kim YJ. Piceatannol inhibits melanogenesis by its antioxidative actions. Biol Pharm Bull 2007; 30: 2007-2011.

25) Jung HJ, Choi DC, Noh SG, Choi H, Choi I, Ryu IY, Chung HY, Moon, HR. New Benzimidazothiazolone Derivatives as Tyrosinase Inhibitors with Potential Anti-Melanogenesis and Reactive Oxygen Species Scavenging Activities. Antioxidants 2021; 10: 1078.

26) Sobanska M, Scholz S, Nyman AM, Cesnaitis R, Gutierrez AS, Kluver N, Kuhne R, Tyle H, De Knecht J, Dang Z, Lundbergh I, Carlon C, De Coen W. Applicability of the fish embryo acute toxicity (FET) test (OECD 236) in the regulatory context of Registration, Evaluation, Authorisation, and Restriction of Chemicals (REACH). Environ. Toxicol Chem 2018; 37: 657-670.

27) Wang Y, Liu W, Yuan B, Yin X, Li Y, Li Z, Cui J, Yuan X, Li Y. The Application of Methylprednisolone Nanoscale Zirconium-Porphyrin Metal-Organic Framework (MPS-NPMOF) in the Treatment of Photoreceptor Degeneration. Int J Nanomedicine 2019; 14: 9763-9776.

28) Love MI, Huber W, Anders S. Moderated estimation of fold change and dispersion for RNA-seq data with DESeq2. Genome Biol 2014; 15: 550.

29) Sundaram MK, Khan MA, Alalami U, Somvanshi P, Bhardwaj T, Pramodh S, Raina R, Shekfeh Z, Haque S, Hussain A. Phytochemicals induce apoptosis by modulation of nitric oxide signaling pathway in cervical cancer cells. Eur Rev Med Pharmacol Sci 2020; 24: 11827-11844.

30) Zhu G, Mei L, Vishwasrao HD, Jacobson O, Wang Z, Liu Y, Yung BC, Fu X, Jin A, Niu G, Wang Q, Zhang F, Shroff H, Chen X. Intertwining DNA-RNA nanocapsules loaded with tumor neoantigens as synergistic nanovaccines for cancer immunotherapy. Nat Commun 2017; 8: 1482.

31) Hong SS, Choi JH, Lee SY, Park YH, Park KY, Lee JY, Kim J, Gajulapati V, Goo JI, Singh S, Lee K, Kim YK, Im SH, Ahn, SH, Rose-John S, Heo TH, Choi Y. A Novel Small-Molecule Inhibitor Targeting the IL-6 Receptor beta Subunit, Glycoprotein 130. J Immunol 2015; 195: 237-245.

32) Iacobucci I, Li Y, Roberts KG, Dobson SM, Kim JC, Payne-Turner D, Harvey RC, Valentine M, Mccastlain K, Easton J, Yergeau D, Janke LJ, Shao Y, Chen IM, Rusch M, Zandi S, Kornblau SM, Konopleva M, Jabbour E, Paietta EM, Rowe JM, Pui CH, Gastier-Foster J, Gu Z, Reshmi S, Loh ML, Racevskis J, Tallman MS, Wiernik PH, Litzow MR, Willman CL, Mcpherson JD, Downing JR, Zhang J, Dick JE, Hunger SP, Mullighan CG. Truncating Erythropoietin Receptor Rearrangements in Acute Lymphoblastic Leukemia. Cancer Cell 2016; 29: 186-200.

33) Sims NA. The JAK1/STAT3/SOCS3 axis in bone development, physiology, and pathology. Exp Mol Med 2020; 52: 1185-1197.

34) Arnold CE, Whyte CS, Gordon P, Barker RN, Rees AJ, Wilson HM. A critical role for suppressor of cytokine signalling 3 in promoting M1 macrophage activation and function in vitro and in vivo. Immunology 2014; 141: 96-110.

35) Zhou D, Chen L, Yang K, Jiang H, Xu W, Luan J. SOCS molecules: the growing players in macrophage polarization and function. Oncotarget 2017; 8: 60710-60722.

36) Han H, Kim Y, Mo H, Choi SH, Lee K, Rim YA, Ju JH. Preferential stimulation of melanocytes by M2 macrophages to produce melanin through vascular endothelial growth factor. Sci Rep 2022; 12: 6416.

37) Du Q, Fu YX, Shu AM, Lv X, Chen YP, Gao YY, Chen J, Wang W, Lv GH, Lu JF, Xu HQ. Loganin alleviates macrophage infiltration and activation by inhibiting the MCP-1/CCR2 axis in diabetic nephropathy. Life Sci 2021; 272: 118808.

38) Zhang J, Wang C, Wang H, Li X, Xu J, Yu K. Loganin alleviates sepsis-induced acute lung injury by regulating macrophage polarization and inhibiting NLRP3 inflammasome activation. Int Immunopharmacol 2021; 95: 107529.

39) Chunhakant S, Chaicharoenpong C. Antityrosinase, Antioxidant, and Cytotoxic Activities of Phytochemical Constituents from Manilkara zapota L. Bark. Molecules 2019; 24: 2798.

40) Swope VB, Abdel-Malek Z, Kassem LM, JJ Nordlund. Interleukins 1 alpha and 6 and tumor necrosis factor-alpha are paracrine inhibitors of human melanocyte proliferation and melanogenesis.J Invest Dermatol 1991; 96: 180-185.

41) Choi H, Ahn S, Lee BG, Chang I, Hwang JS. Inhibition of skin pigmentation by an extract of Lepidium apetalum and its possible implication in IL-6 mediated signaling. Pigment Cell Res 2005; 18: 439-446.

42) Kamaraju AK, Bertolotto C, Chebath J, Revel M. Pax3 down-regulation and shut-off of melanogenesis in melanoma B16/F10.9 by interleukin-6 receptor signaling. J Biol Chem 2002; 277.

43) Heinrich PC, Behrmann I, Haan S, Hermanns HM, Muller-Newen G, Schaper F. Principles of interleukin (IL)-6-type cytokine signalling and its regulation. Biochem J 2003; 374.

44) Chen W, Yuan H, Cao W, Wang T, Chen W, Yu H, Fu Y, Jiang B, Zhou H, Guo H, Zhao X. Blocking interleukin-6 trans-signaling protects against renal fibrosis by suppressing STAT3 activation. Theranostics 2019; 9: 3980-3991.

45) Sims, NA. The JAK1/STAT3/SOCS3 axis in bone development, physiology, and pathology. Exp Mol Med 2020; 52: 1185-1197.

46) Kortylewski M, Heinrich PC, Mackiewicz A, Schniertshauer U, Klingmuller U, Nakajima K, Hirano T, Horn F, Behrmann I. Interleukin-6 and oncostatin M-induced growth inhibition of human A375 melanoma cells is STAT-dependent and involves upregulation of the cyclin-dependent kinase inhibitor p27/Kip1. Oncogene 1999; 18: 3742-3753.

47) Lacreusette A, Nguyen JM, Pandolfino MC, Khammari A, Dreno B, Jacques Y, Godard A, Blanchard F. Loss of oncostatin M receptor beta in metastatic melanoma cells. Oncogene 2007; 26: 881-892.

48) Swoboda A, Soukup R, Eckel O, Kinslechner K, Wingelhofer B, Schorghofer D, Sternberg C, Pham H, Vallianou M, Horvath J, Stoiber D, Kenner L, Larue L, Poli V, Beermann F, Yokota T, Kubicek S, Krausgruber T, Rendeiro AF, Bock C, Zenz R, Kovacic B, Aberger F, Hengstschlager M, Petzelbauer P, Mikula M, Moriggl R. STAT3 promotes melanoma metastasis by CEBP-induced repression of the MITF pathway. Oncogene 2021; 40: 1091-1105.